

Spatial Mapping of Soil Depth, Coarse Fragments and Textural Classes of Tamil Nadu Using Digital Soil Mapping Approach

B Kalaiselvi (✉ kalaimitra15@gmail.com)

ICAR-National Bureau of Soil Survey and Land Use Planning <https://orcid.org/0000-0002-1452-7255>

S. Dharumarajan

ICAR-National Bureau of Soil Survey and Land Use Planning

M. Lalitha

ICAR-National Bureau of Soil Survey and Land Use Planning

R. Srinivasan

ICAR-National Bureau of Soil Survey and Land Use Planning

R. Vasundhara

ICAR-National Bureau of Soil Survey and Land Use Planning

Amar Suputhra

ICAR-National Bureau of Soil Survey and Land Use Planning

Rajendra Hegde

ICAR-National Bureau of Soil Survey and Land Use Planning

Research Article

Keywords: Spatial distribution, digital soil mapping, environmental covariates, soil properties, random forest model.

Posted Date: June 16th, 2021

DOI: <https://doi.org/10.21203/rs.3.rs-596172/v1>

License: © ⓘ This work is licensed under a Creative Commons Attribution 4.0 International License.

[Read Full License](#)

23 distribution of soil depth, coarse fragments (CF) and soil textural classes over 0.13 M sq.km
24 area of Tamil Nadu state. About 2100 samples were used for the prediction of soil
25 properties using random forest model (RF). Out of which, 80 per cent samples were used
26 for training and 20 percent samples were used for testing. Different environmental
27 covariates such as digital elevation model outputs, landsat data and bioclimatic variables
28 were related to predict the soil properties. The predicted soil depth and CF ranged from 46-
29 200 cm and 1-42 per cent respectively. The RF model performed well by explaining the
30 variability (R^2) of 43% for soil depth and 21% for coarse fragments with RMSE of 38 cm
31 and 13%, respectively. The RF classifier classified the soil textural classes with 64% overall
32 accuracy and 43% kappa index. Variable importance ranking of Random forest model
33 showed that elevation, MrVBF are the important predictors used for prediction of soil
34 depth and CF, whereas remote sensing vegetation indices such as NDVI, EVI were acted as
35 primary variable for prediction of soil textural classes. In this study, 250 m resolution
36 detailed soil depth, CF and textural class maps were prepared which will be useful for
37 different environmental modeling and proper agricultural management purposes.

38 **Keywords:** Spatial distribution, digital soil mapping, environmental covariates, soil
39 properties, random forest model.

40 **Declarations**

41 **Conflicts of interest/Competing interests:** The authors declare that they have no
42 potential competing financial interests or personal relationships that could have appeared
43 to influence the work reported in this paper.

44 **Availability of data and material:** The data that utilized for the study available from the
45 corresponding-author upon reasonable request.

46

47

48

49 **Spatial mapping of soil depth, coarse fragments and textural classes of Tamil Nadu**
50 **using Digital soil mapping approach**

51 **Kalaiselvi, B*, S. Dharumarajan, M. Lalitha, R. Srinivasan, R. Vasundhara, Amar Suputhra and**
52 **Rajendra Hegde**

53 ***Corresponding author: kalaimitra15@gmail.com**

54 **ICAR-National Bureau of Soil Survey and Land Use Planning, Regional Centre, Hebbal, Bangalore,**
55 **Karnataka, India**

56 **Abstract**

57 Knowledge on spatial distribution of soil depth, coarse fragments and texture are crucial
58 for land resource management and environmental soil modeling. Digital soil mapping
59 approach helps in prediction of spatial soil information by establishing the relationship
60 between soil and environmental covariates. In the present study, we assessed spatial
61 distribution of soil depth, coarse fragments (CF) and soil textural classes over 0.13 M sq.km
62 area of Tamil Nadu state. About 2100 samples were used for the prediction of soil
63 properties using random forest model (RF). Out of which, 80 per cent samples were used
64 for training and 20 percent samples were used for testing. Different environmental
65 covariates such as digital elevation model outputs, landsat data and bioclimatic variables
66 were related to predict the soil properties. The predicted soil depth and CF ranged from 46-
67 200 cm and 1-42 per cent respectively. The RF model performed well by explaining the
68 variability (R^2) of 43% for soil depth and 21% for coarse fragments with RMSE of 38 cm
69 and 13%, respectively. The RF classifier classified the soil textural classes with 64% overall
70 accuracy and 43% kappa index. Variable importance ranking of Random Forest model
71 showed that elevation, MrVBF are the important predictors used for prediction of soil

72 depth and CF, whereas remote sensing vegetation indices such as NDVI, EVI were acted as
73 primary variable for prediction of soil textural classes. In this study, 250 m resolution
74 detailed soil depth, CF and textural class maps were prepared which will be useful for
75 different environmental modeling and proper agricultural management purposes.

76 **Keywords:** Spatial distribution, digital soil mapping, environmental covariates, soil
77 properties, random forest model.

78

79 **Introduction**

80 With increasing need for site-specific management in agriculture, the planners and
81 researchers require spatially continuous soil information at higher resolution for better
82 representation, resource assessment, spatial crop planning, land management and effective
83 policy making at regional and national level (McBratney et al. 2003). Spatial pattern of soil
84 depth influences soil moisture, plant available water content, nutrient capacity, runoff
85 generation (Gribb et al. 2009) and biological productivity (Gessler et al. 1995). Similarly,
86 soil texture plays a key role in nutrient retention (Kettler et al. 2001), soil aeration and
87 porosity, soil aggregation and structure development (Carrizo 2015), soil organic carbon
88 and soil quality (Kong et al. 2009), soil water transportation, soil degradation (Hillel 1980)
89 and soil productivity (Katerji & Mastrorilli 2009). These soil properties are also act as
90 important criteria in grouping the soil series for similar management purpose, land
91 suitability classes (Thompson et al. 2012) and involve in soil taxonomic classifications (Soil
92 Survey Staff 2014). Assessing spatial distribution of soil depth and coarse fragments is
93 laborious, difficult to measure practically as they are highly variable spatially (Wilding
94 1985).

95 Need for spatially seamless soil information dealt by prediction of soil properties by
96 the concept of digital soil mapping which predicts the dependent soil properties (Florinsky
97 et al. 2002) using the interrelationship between environmental covariates (DEM, climatic
98 parameters, remote sensing imageries) (McBratney et al. 2003) and legacy soil information
99 (Akpa et al. 2014) through numerical, statistical and geostatistical models (Minasny and
100 McBratney 2016). It takes the advantage of ability to produce uncertainty and able to
101 update when new data collected (Lagacherie and McBratney 2007). Spatial patterns in soil

102 properties (soil depth, CF and texture) are resultant of complex interactions of different
103 factors such as geomorphic positions, topography, parent material, climate, weathering
104 rate, vegetation cover, lithology (Kuriakose et al. 2009), biological, chemical and physical
105 processes (Jenny 1941; Odeh et al. 1991). Thus, the environmental covariates related with
106 soil development selected for establishing the DSM models such as legacy soil data (S),
107 climatic information (C), Vegetation/landuse (O), derivatives of digital elevation models
108 (R), lithology (P) and geographic co-ordinates (N) (Minasny and McBratney 2016).

109 Tsai et al. (2001) used linear soil landscape regression model to map soil depth in
110 Taiwan and estimated the spatial column thickness with RMSE of 16.13 cm. Tesfa et al.
111 (2009) developed statistical models for prediction of soil depth over complex terrain in
112 DCE watershed, USA (28 sq.km of 819 sub-watersheds) and found that with increasing
113 complexity of variabilities, RF outperforms as it is robust against overfitting. Kuriakose et
114 al. (2009) predicted soil depth with maximum capturable variability of 52% (R^2) in part of
115 Western ghats, Kerala. Mehnatkesh et al. (2013) identified the relationship between soil
116 depth and topographic variables (slope, WI, catchment area and sediment transport index)
117 using MLR and explained 76% total variability of soil depth. Bonfatti et al. (2016) used
118 multilinear regression model in Southern Brazil (8118 ha) and predicted soil depth with R^2 ,
119 RMSE and CCC of 0.43, 34.8 cm and 0.59 respectively. Lacoste et al. (2014) investigated soil
120 depth for a region in France of approximately 5,40,000 km² and predicted the soil depth
121 with R^2 and RMSE values between 50–58% and 35–39 cm. Vaysse and Lagacherie (2017)
122 attempted to predict soil depth of Languedoc-Roussillon region, France and could capture
123 the maximum variability of $R^2= 23\%$ with RMSE of 34 cm. In India, Dharumarajan et al.

124 (2020a) prepared 250 m resolution soil depth map of Karnataka using Regression kriging
125 and QRF model which could explain maximum variability of 30% (R^2) and 34 cm (RMSE).

126 Mosleh et al. (2016) used different Machine learning techniques (ANN, BRT, GLM
127 and MLR) and found CF with 0.07 R^2 with RMSE of 3.2-3.7 which had high variability about
128 260%. Similarly, Vaysse and Lagacherie (2015) evaluated simulation models, RFM and
129 kriging approaches to coarse fragments and could capture only 4% variability of coarse
130 fragments. Nussbaum et al. (2018) found that RF model performed better in prediction of
131 soil gravel content with minimal RMSE of 2.64%.

132 Few studies have been conducted in India to map soil textural classes either through
133 prediction of sand, silt and clay particle size fractions (PSF) (Mitran et al. 2018;
134 Dharumarajan et al. 2020) or categorical classes (Dharumarajan et al. 2020b). Many
135 researches focused on PSF prediction for hydrological modelling, SOC stock estimation and
136 textural class mapping using textural triangles (Akpa et al. 2014; Chagas et al. 2016;
137 Mehrabi-Gohari et al. 2019; Zeraatpisheh et al. 2019; Dharumarajan et al. 2020b). RF
138 classifier algorithms outperformed in classification of soil taxonomic classes (Silva et al.
139 2019; Boroujeni et al. 2020), parent material (Heung et al. 2014), land suitability (Senagi et
140 al. 2017) etc. Ließ et al. (2012) found the maximum efficacy of RF model over Regression
141 Tree in PSF prediction (30-40% R^2). Vaysse and Lagacherie (2015) predicted PSF using RF
142 with 33-35% R^2 of sand, 31-35% R^2 of clay and 23-29% R^2 of silt content. Camera et al.
143 (2017) reported that random forest classifier was more remarkable than MLR in soil
144 texture classification. Zhang et al. (2020) compared five different models for the
145 classification of soil texture class and found that random forest classifier performed
146 significantly with overall accuracy of 65 per cent and profound improvement in kappa

147 index of 21 per cent. Abraham et al. (2020) predicted soil particle size fractions using the
148 Random Forest algorithm to get soil textural classes and got the highest overall accuracy of
149 84.70 percent compared to other models with kappa index of 55-70 percent.

150 After inception of GlobalSoilMap project, many researches focused on spatial
151 mapping of soil properties worldwide (Arrouays et al. 2014). In India, very limited
152 attempts only made in digital soil mapping (Sreenivas et al. 2016; Dharumarajan et al.
153 2017, 2019 & 2020; Reddy et al. 2021). Accurate prediction of soil properties would help in
154 crop productivity and comprehensive land management especially ecological, crop
155 suitability and hydrological modelling. With this context, an exploratory study was
156 conducted to map soil depth, CF and texture of Tamil Nadu experiencing semiarid climate
157 using Random Forest model techniques.

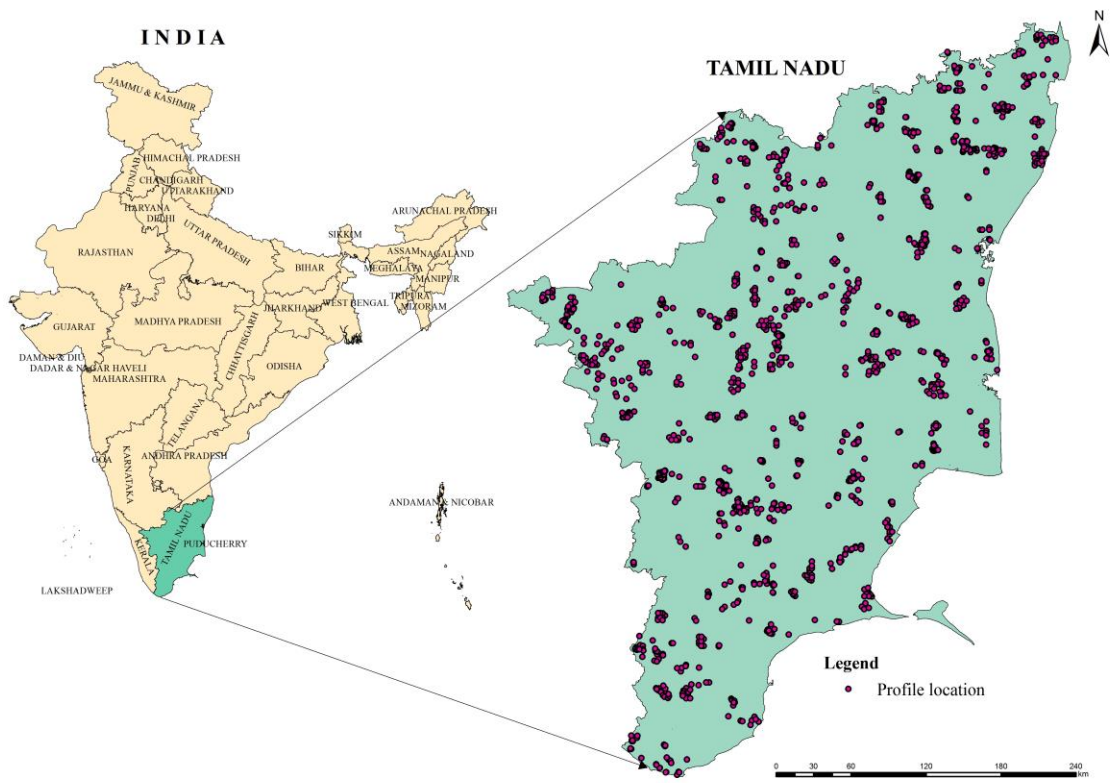
158

159 **Materials and Methods:**

160 ***Study Area***

161 Tamil Nadu is the south most state in India with 130058 sq.km area extended
162 between 8°5' and 13°35' N and 76°15' and 80°12' E which accounts for 3.96 percent of the
163 total geographical area (TGA) of the country (Fig.1). Tamil Nadu state has been divided into
164 three physiographic units namely South deccan plateau (uplands), Hill ranges and Coastal
165 Plains (Inland plain and Marine plain) (Natarajan et al. 1997). The geological formations of
166 study area are dominant with Precambrian granitic, pink gneiss and charnockite followed
167 by Pleistocenic alluvium and in someparts Pliocene sandstone. Tamil Nadu comes under
168 semiarid agro-eco region which receives bi-model rainfall ie., 48 % from NEM and 32%
169 from SWM. Mean minimum and maximum temperatures ranged between 21.6°C-31.8°C.

170 Dominant soils are Inceptisols (50%), Alfisols (30%), followed by Vertisols (7%), Entisols
171 (6%) and Ultisols (1%) and negligible areas of Mollisols (Natarajan et al. 1997). Major
172 crops being cultivated are Paddy, Pulses, Groundnut, Sugarcane, Cotton, Coconut, fruit and
173 vegetable crops.



174

175

Fig.1. Study area with profile locations

176 ***Sampling Methodology***

177 Soils studied during soil resource mapping (SRM) of Tamil Nadu at 1:250,000 scale
178 (1989–1999) and soils studied by Tamil Nadu state soil survey department and other
179 ICAR-NBSS&LUP projects are collected and organized for mapping of soil depth, coarse
180 fragments and texture in Tamil Nadu. The geospatial information of the soils studied during
181 soil resource mapping were limited with degree-minutes which were again assigned with

182 specific coordinate pertained to the village information. A total of 2119 soil profiles were
183 used for depth prediction study after removing the outliers whereas 2105 surface soil
184 samples were used for coarse fragments and texture class mapping. While using the soil
185 textural classes for spatial mapping, neighbouring soil textural classes are merged into
186 broader classes such as clay and sandy clay into clay (C), clay loam and sandy clay loam in
187 to loam (L) and loamy sand and sandy loam into sandy (S) textural classes based on the
188 earlier studies proven that more number of soil classes with less frequencies may result in
189 significant decrease in prediction accuracy (Lagacharie et al. 2019; Boroujeni et al. 2020).

190 **Environmental co-variates:**

191 Digital elevation model (DEM) of 30 m resolution obtained from shuttle radar
192 topography mission (SRTM) was used to derive different topographic derivatives such as,
193 elevation, slope, aspect, topographic position index (TPI), topographic wetness Index
194 (TWI), LS factor, Multi-resolution Index of Valley Bottom Flatness (MrVBF) and multi-
195 resolution ridge top flatness (MrRTF) as topography is the main soil forming factor in semi-
196 arid regions (Mehnatkesh et al. 2013). Remote sensing variables such as, LISS III band data
197 (1-4), normalized difference vegetation index (NDVI) and enhanced vegetation index (EVI)
198 were also used to relate with the soil properties. Annual mean rainfall, maximum mean
199 temperature (Tmax) and minimum mean temperature (Tmin) are used to represent
200 climate in the models. The bio-climatic variables (19) such as isothermality, precipitation of
201 driest month, precipitation of wettest month, precipitation seasonality and mean diurnal
202 range were also included as environmental covariates for soil properties prediction.
203 Correlation between the soil properties and the environmental co-variates was analyzed

204 using pearson correlation coefficient analysis with confidence level of 95%. Soil properties
 205 prediction methodology presented in Fig. 2.

206 **Table 1. Different covariates used in the model**

Predictor	Source	Resolution
Elevation (m)	SRTM DEM	30 m
Slope (%)	SRTM DEM	30 m
Aspect	SRTM DEM	30 m
TPI	SRTM DEM	30 m
TWI	SRTM DEM	30 m
Plan curvature	SRTM DEM	30 m
LS-factor	SRTM DEM	30 m
MrVBF	SRTM DEM	30 m
MrRTF	SRTM DEM	30 m
NDVI	MOD13Q1(2011-2015)	250m _16
EVI	MOD13Q1(2011-2015)	days
LISS-III	4 bands	26 m
Precipitation (mm)	WorldClim2	10 min
Minimum temperature (Tmin) (°C)	WorldClim2	10 min
Maximum temperature (Tmax) (°C)	WorldClim2	10 min
Isothermality	WorldClim2	10 min
Precipitation of driest month (mm)	WorldClim2	10 min
Precipitation of wettest month (mm)	WorldClim2	10 min
Precipitation seasonality	WorldClim2	10 min

207	Mean diurnal range	WorldClim2	10 min
208	(°C)		

209 ***Random forest model:***

210 Random Forest model (RFM) is an ensemble of decision trees which considers each
 211 individual tree's decision to predict and classify the soil properties in addition, it can rank
 212 the variables based on their significance in prediction (Breiman 2001). RF model tuned
 213 depending on the number of trees to be grown (ntree), number of variables used to split
 214 the nodes (mtry) and minimum number of samples at each node (nmin). Random forest
 215 model is insensitive to noisy, huge and missing dataset which can handle both quantitative
 216 and categorical dataset by regression and classification algorithm (Dharumarajan et al.
 217 2017). Statistical software R of randomForest package (Version R 4.0.5) was used to
 218 establish the relationship between environmental variables (R Development Core Team
 219 2012).

220 **Model prediction performance:**

221 For calibration of the prediction model, 80% of soil depth and CF datasets were used
 222 and 20% remaining dataset was used for validation dataset and based on the 50 iterations
 223 the performance of the models was evaluated. Model prediction performance was
 224 evaluated using coefficient of determination (R²), Lin's concordance correlation coefficient
 225 (CCC), root mean square error (RMSE) and mean error (bias) of the validation datasets
 226 (Mitran et al., 2018). The value of R² and CCC nearing 1 and RMSE to 0, indicates the good
 227 prediction performance of the model (Dharumarajan et al. 2017).

228
$$R2 = 1 - \frac{\sum_{i=1}^n (pi - oi)^2}{\sum_{i=1}^n (oi - \bar{oi})^2}$$

229

230

$$ME = \frac{1}{n} \sum_{i=1}^n (oi - pi)$$

231

$$RMSE = \sqrt{\frac{1}{n} \sum_{i=1}^n (oi - pi)^2}$$

232

Where, pi and oi are predicted and observed values, pi and oi are means of predicted and

233

observed values.

234

Lin's Concordance correlation coefficient

235

$$CCC (\rho_c) = \frac{2\rho\sigma_o \sigma_p}{\sigma_o^2 + \sigma_p^2 + (\mu_o - \mu_p)^2}$$

236

μ_o and μ_p are the means of observed and predicted values and σ_o^2 and σ_p^2 are

237

corresponding variance ρ is Pearson correlation coefficient between observed and

238

predicted values.

239

Performance evaluation of RF classifier algorithm:

241

The performance of the RF classifier determined based on overall accuracy, and

242

kappa index.

243

Overall accuracy:

244

Percentage of data correctly classified in the validation set is calculated as Overall

245

accuracy. Overall accuracy (OA) is used to measure the effectiveness of the model which is

246

shown as below,

247

$$OA = \sum_{i=1}^n \frac{X_{ii}}{N}$$

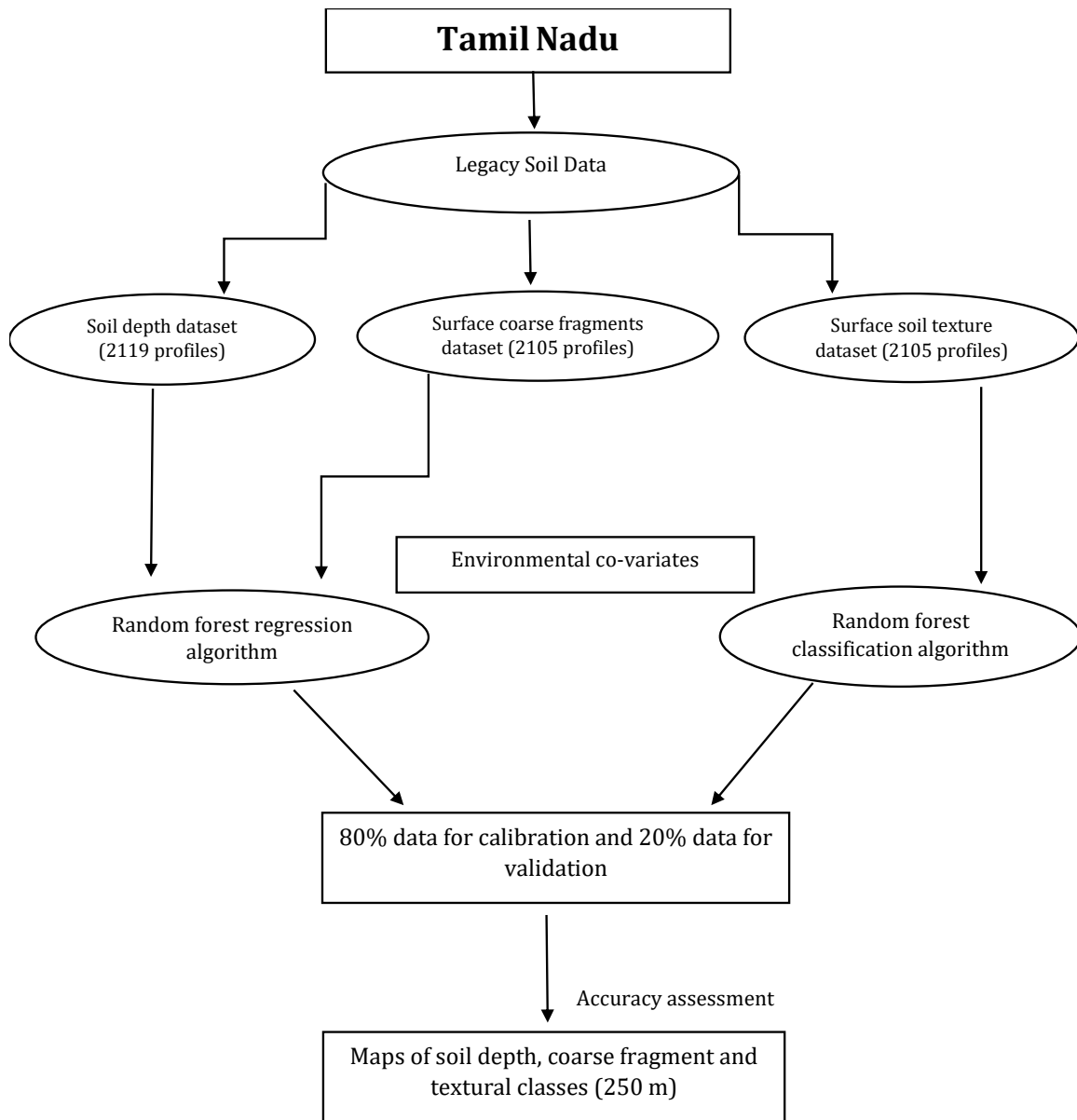
248 Where n is the number of columns or rows of error matrix, X_{ii} is the classes predicted
249 properly, and N is the total number of observations (Byrt et al. 1993).

250 ***Kappa index:***

251 Kappa index is the degree to which classification outcome is superior than the
252 outcome of random classification (Cohen 1960). Kappa index >0.80 , $0.4-0.8$ and <0.4
253 indicates the strong, moderate and poor agreements of classification, respectively
254 (Congalton and Green 1998).

255 ***Uncertainty analysis:***

256 The lack of reality assurance in prediction is considered as uncertainty (Heuvelink,
257 2013) and its estimation along with prediction is important for assessing the risk in
258 decision making. The uncertainty of the prediction was quantified by computing upper
259 (95% quantile) and lower confidence (5% quantile) interval limits on the prediction map
260 (Viscarra Rossel et al. 2014) which indicates that 90% of the time, an observed value will
261 fall with in this prediction interval (Malone et al. 2014). The uncertainty for classifier
262 algorithm is evaluated by error/confusion matrix (Boroujeni et al. 2020) which compares
263 the measured and predicted soil classes and checks whether the categorization is
264 satisfactory (Story and Congalton 1986). Confusion index/ error classification values vary
265 from 0 to 1, of which larger values indicate higher uncertainty.



266

267

268

Fig. 2. Methodology Flow Chart

269 **Result and Discussion:**

270 ***Descriptive statistics:***

271 Summary statistics of soil depth and coarse fragments are given in Table. 2. Soil
272 depth varied from 9-217 cm with mean of 119 ± 51 cm. Soil depth was skewed positively
273 with negative kurtosis and the co-efficient of variation was 42.5 percent which indicates
274 the high variability of soil depth in the study area. Similar results are in concordance with
275 Kuriakose et al. (2009) and Dharumarajan et al. (2020a). Coarse fragments varied from
276 non-gravelly (<15%) to very gravelly (80%) with positive skewness and kurtosis which
277 shows the assymetrical distribution of CF. The very high variability (Wilding 1985) of
278 coarse fragments (CV-135%) was recorded due to differences in landscape,
279 transportability of soil particles and geographical dissimilarity (Tola et al. 2017). The
280 variability of soil properties might attributed to the variability in topography and soil
281 formation (Grimm et al. 2008). Correlation analysis has registered significant relationship
282 between soil depth and coarse fragments with environmental variables (Table. 3). Soil
283 depths were positively correlated with MRRTF ($r=0.10^{**}$), MRVBF ($r=0.20^{**}$), precipitation
284 ($r=0.24^{**}$) and minimum temperature (T_{min}) ($r=0.15^{**}$). It was negatively correlated with
285 elevation ($r=-0.14^{**}$), TWI ($r=-0.13^{**}$) and with satellite band data. In contrast to soil
286 depth, coarse fragments shown significant positive relationship with elevation ($r=0.06^{**}$),
287 TWI ($r=0.13^{**}$) and band data and negative correlation with MRRTF ($r=-0.08^{**}$), MRVBF
288 ($r=-0.15^{**}$), maximum (T_{max}) and minimum temperature (T_{min}). With increasing slope
289 and elevation, the soil depth and coarse fragments shown negative and positive
290 relationship respectively due to erosional soil loss on slope gradients (Tsai et al. 2001;
291 Florinsky et al. 2002). This correlation study shows indirectly that coarse fragments of

292 valley (alluvial plains) are mere negligible as the depositional soils are devoid of coarse
293 fragments (Dharumarajan et al. 2021). Soil textural classes were recorded from 2105
294 surface samples in Tamil Nadu and classified into clay (464), loam (641) and sandy (1000)
295 textural classes. Among the studied soils, predominant soil textural class is sandy soil that
296 occupies about 48% followed by loamy soils (31%).

297 ***Performance of RF prediction model:***

298 The performance of the model was evaluated with average performance over 50
299 iterations using the accuracy indicators like R^2 , RMSE and bias given in Table 4. The result
300 shown that the soil depth was predicted with the explained variability of $R^2=0.43\pm0.04$ and
301 RMSE of 38 cm. The concordance value for the prediction was 0.612 ± 0.03 that confirms
302 that the moderately good performance of the model (Dharumarajan et al. 2017). The
303 performance of the Random Forest model was comparatively better than the QRF model
304 used in Karnataka soil depth mapping which could only explain 17% variability (R^2)
305 (Dharumarajan et al. 2020a). In African continent, Hengl et al. (2021) predicted soil depth
306 to bedrock using 30 m resolution co-variables using 28054 sample data and predicted depth
307 with 0.43 R^2 ; 41.3 cm RMSE and 0.73 CCC with ensemble of RF, XG boost, deep net, Cubist
308 and GLM net. The prediction of coarse fragments shown that the model could find the
309 variability of 21 per cent ($R^2=0.21$) with 13% RMSE. Compared to soil depth, the bias is
310 higher for coarse fragment prediction. The prediction of CF by RFM is quite low which
311 might be due to high terrain variability and minimal dataset of gravelly soils (Mosleh et al.
312 2016). Hengl et al. (2004) predicted coarse fragments using SVM with medium level of
313 validity. With regard to soil surface textural classification, the random forest classifier
314 classified the textural class with overall accuracy and kappa index of 63.8% and 41.5%,

315 respectively with confidence interval of 0.59-0.68. This short range of prediction interval
316 indicates the better performance of RF classifier. The performance of RF model is similar to
317 Dharumarajan et al. (2020b) who mapped spatial and vertical (GlobalSoilMap depth
318 specification) textural class map of Andhra Pradesh by predicting PSF and could classify
319 the textural classes with overall accuracy and kappa coefficient of 52-65% and 42-47%
320 respectively. Similar results were obtained from soil textural classification using Landsat-5
321 TM images reported with over all accuracy of around 58-64% (Dematte et al. 2016). Zhang
322 et al. 2020) signified the performance of RF in soil textural classification with profound
323 improvement in reduction of error with increased kappa index of 0.21 by comparing 5
324 different ML models. Boroujeni et al. (2020) classified WRB soil classes using RF model and
325 resulted with 0.73 OA at first level with less confusion index. The mean of confusion matrix
326 obtained by running 50 RF models given in Table 6. In which, only 187 soils only correctly
327 classified as clay out of 464 soil, similarly 275 soils only classified as loamy out of 641.
328 Despite, about 60 per cent of the soils were classified to the correct class (Sandy texture).
329 The error matrix shows (Table 6) that the classification of sandy classes (error= 0.261) is
330 much better than other class (clay= 0.497; loam= 0.464) with respect to error estimates.
331 The results are in concordance with the previously documented studies that classes with
332 lower sampling frequencies were modeled less accurately (e.g., Lagacherie et al. 2019;
333 Boroujeni et al. 2020).

334 ***Importance of variables:***

335 The variables that contribute substantial for prediction of soil properties are
336 assessed by Random Forest model. Fig.3 shows the variable importance ranking of RFM for
337 prediction of soil depth, CF and textural classes. Derivatives of digital elevation models/

338 topographic variables such as elevation, MRVBF, MRRTF are the primary variables involves
339 in prediction of soil depth and coarse fragment contents (Adhikari et al. 2013; Lu et al.
340 2019). Some climatic (Tmax) and bioclimatic variables (bio_4) are also bestowed for
341 prediction of soil properties (Malone et al. 2020). Topographic variables were found to be
342 generally more important than the land cover variables in predicting soil depth for this
343 dataset (Tsai et al. 2001; Grimm et al. 2008). Complexity of the environmental variables
344 resulting in variable soil depth (Chan et al. 2019). Similarly, MRVBF and elevation are the
345 prime variables influencing the prediction of coarse fragments. For textural classification,
346 remote sensing indices such as NDVI, EVI, topographical variables (elevation, MRVBF,
347 MRRTF, TWI) (Mehrabi-Gohari et al. 2019) and climatic variables took part in classification
348 of soil textural classes (minimum temperature (Tmin) and Precipitation) (Akpa et al.
349 2014).

350 ***Soil prediction maps:***

351 Summary statistics of the predicted soil properties given in Table 5. Predicted soil
352 depth and CF ranged between 90-195 cm and 0-40% respectively. Skewness and kurtosis
353 of the predicted coarse fragments indicates the presence of extreme values which is
354 reflected in coefficient of variation (CV%-142%), whereas, the predicted soil depth did not
355 register much variability (CV%-11.4%). Predicted soil depth map (Fig. 4a) shows that the
356 depth ranged between 46 and 200 cm and the deeper soils occurring on western ghat
357 (western side) attributed to climate and vegetational influence on soil development
358 (Dharumarajan et al. 2020a) and valley bottom (eastern and south-eastern part) of Tamil
359 Nadu due to the deposition of soil particles from higher elevation to lower elevation
360 (Bonfatti et al. 2016). Spatial variability of soil depth attributed to parent material,

361 relief/topography and climate (Shivaprasad et al. 1998). Rudiyanto et al. (2016) suggested
362 that improved sampling strategies and machine learning approaches can increase the
363 accuracy of soil depth prediction. Coarse fragments map varied with 1 to 42 per cent of CF
364 (Fig. 4c). Higher CF content was noticed in western and northwestern part of Tamil Nadu
365 (Western ghats and Tamil Nadu uplands). Contradict to depth distribution, CF recorded
366 high in uplands and low in alluvial/coastal plains owing to runoff losses of soil finer
367 particles. According to textural class map (Fig. 5), the Tamil Nadu surface soils are
368 dominated with sandy texture (Sandy loam and loamy sand), followed by clayey (clay,
369 sandy clay) and loamy soils (clay loam and sandy clay loam). Clayey soils distributed in
370 eastern and southern coastal part of Tamil Nadu, whereas, sandy soils distributed in
371 northern and central part of Tamil Nadu. Variation of textural classes shows the transition
372 of clay particles through fluvial movement from upland to lower elevation of eastern and
373 south eastern part of Tamil Nadu with high clayey soils (Dharumarajan et al. 2020b).
374 Coarser soil particles found in upper elevation than low lying areas due to the decreased
375 transportability of sand particles (Mashalaba et al. 2020).

376 Uncertainty maps of soil depth (Fig. 4b) manifest that high uncertainty of soil depth
377 was noticed in lowland (coastal) and western ghats region which might be due to local
378 landscape variation. Whereas, the low uncertainty of soil depth was noticed in uplands
379 attributed to the similarity in the landscape and climate. The highest uncertainty of coarse
380 fragments (Fig. 4d) was observed in the Tamil Nadu uplands which might be due to high
381 elevation, erosional variability (Kalaiselvi et al. 2019) and granitic gneiss parent material
382 whereas, the lowest uncertainties were observed in the coastal and low lying lands
383 attributed to the non-gravelliness of depositional soils (Dharumarajan et al. 2021).

384 Regardless, the predicted soil maps can help in assessing the physical constraints for crop
385 growth (Vagen et al. 2016), and used to find the suitable crops to cultivate, optimal
386 fertilizer and other management aspects.

387 **Conclusion:**

388 In the present study, digital soil depth, coarse fragments and textural class maps
389 were prepared using RF model. The result shown that the interrelationship between
390 covariates could explain 43 and 21 per cent of soil depth and coarse fragments variability
391 respectively. Terrain attributes such as elevation and MrVBF are the main predictors of soil
392 depth and CF, whereas, Remote sensing indices (NDVI and EVI) are the important
393 predictors of soil textural classes. Uncertainty map shows that Tamil Nadu upland soil has
394 high uncertainty of depth prediction than the coastal soils. Surface soil textural mapping
395 also acceptable with overall accuracy of 63.8%. Faster run time and reliable prediction
396 performance of RF model helps in prediction and classification of soil properties. The
397 prediction performance could be improved by incorporating additional covariates such as
398 lithological data etc, increasing sampling density and stratification of dataset for different
399 landscape units.

400 **Declarations**

401 **Conflicts of interest/Competing interests:** The authors declare that they have no
402 potential competing financial interests or personal relationships that could have appeared
403 to influence the work reported in this paper.

404 **Availability of data and material:** The data that utilized for the study available from the
405 corresponding-author upon reasonable request.

406

Table 2. Descriptive statistics of observed soil depth and CF

Parameter	Depth (cm)	CF (%)
Mean	119	11
Minimum	9	0
Maximum	217	80
Std. Dev	50.78	15.0
Skewness	0.02	1.80
Kurtosis	-1.09	3.09
CV (%)	42.5	135

407

408

Table 3. Correlation analysis between covariates and soil properties

Variables	Correlation co-efficient (R)	
	Soil depth	Coarse fragments
Elevation	-0.14**	0.06**
EVI	0.02	-0.00
NDVI	0.01	0.02
TWI	-0.13**	0.13**
LS_Factor	-0.04	0.00
MRRTF	0.10**	-0.08**
MRVBF	0.20**	-0.15**
Plan curvature	0.05*	-0.04
Slope	-0.01	0.01
TPI	-0.01	0.04
Aspect	0.00	-0.02

Prec	0.24**	-0.19**
Minimum temperature (Tmin)	0.15**	-0.07**
Maximum temperature (Tmax)	0.00	0.02
bio_7	-0.24**	0.14**
bio_8	0.02	0.02
bio_6	0.16**	-0.07**
bio_5	-0.01	0.03
bio_4	0.08**	-0.06**
bio_3	-0.20**	0.12**
bio_2	-0.43**	0.25**
bio_19	0.29**	-0.23**
bio_10	0.08**	-0.02
bio_11	0.07**	-0.01
bio_12	0.24**	-0.20**
bio_13	0.24**	-0.20**
bio_14	0.10**	-0.08**
bio_15	0.13**	-0.11**
bio_16	0.30**	-0.25**
bio_17	0.17**	-0.13**
bio_1	0.08**	-0.02
bio_18	-0.08**	0.04
bio_9	0.06**	-0.01
b1_LISS (0.52-0.59 μm)	-0.19**	0.11**
b2_LISS (0.62-0.68 μm)	-0.12**	0.07**
b3_LISS (0.77-0.86 μm)	-0.04*	0.00
b4_LISS (1.55-1.70 μm)	-0.31**	0.18**
*Correlation is significant at the 0.05 level (2-tailed)		
**Correlation is significant at the 0.01 level (2-tailed)		

410

Table 4. Performance of Random Forest model for prediction of soil properties

Soil properties	R ²	Concordance C	RMSE	Mean error
Soil depth (cm)	0.43	0.61	38	0.19
Coarse fragments (%)	0.21	0.42	13	0.44

411

412

413

414

Table 5. Descriptive statistics of predicted soil depth and CF

Parameter	Depth	CF (%)
	(cm)	
Mean	148	2.5
Minimum	90	0
Maximum	195	40
Std. Dev	16.8	3.5
Skewness	0.01	1.66
Kurtosis	-0.31	4.16
CV (%)	11.4	142

415

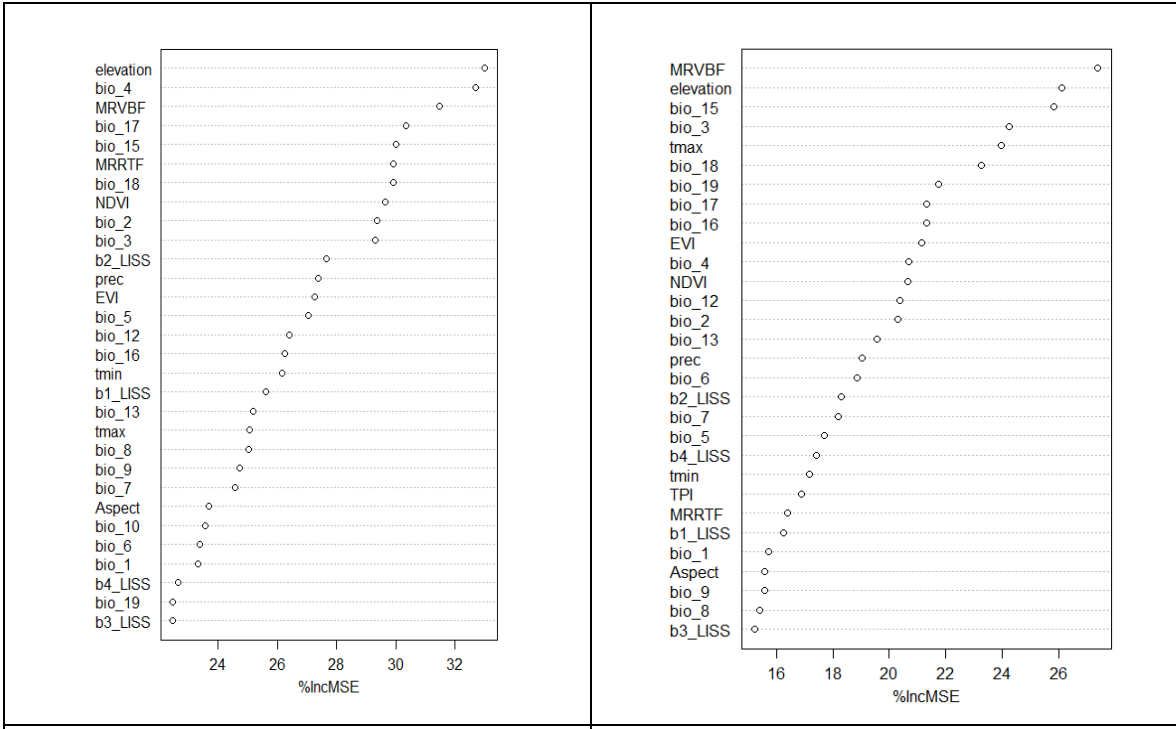
416

Table 6. Confusion matrix of Soil textural classification

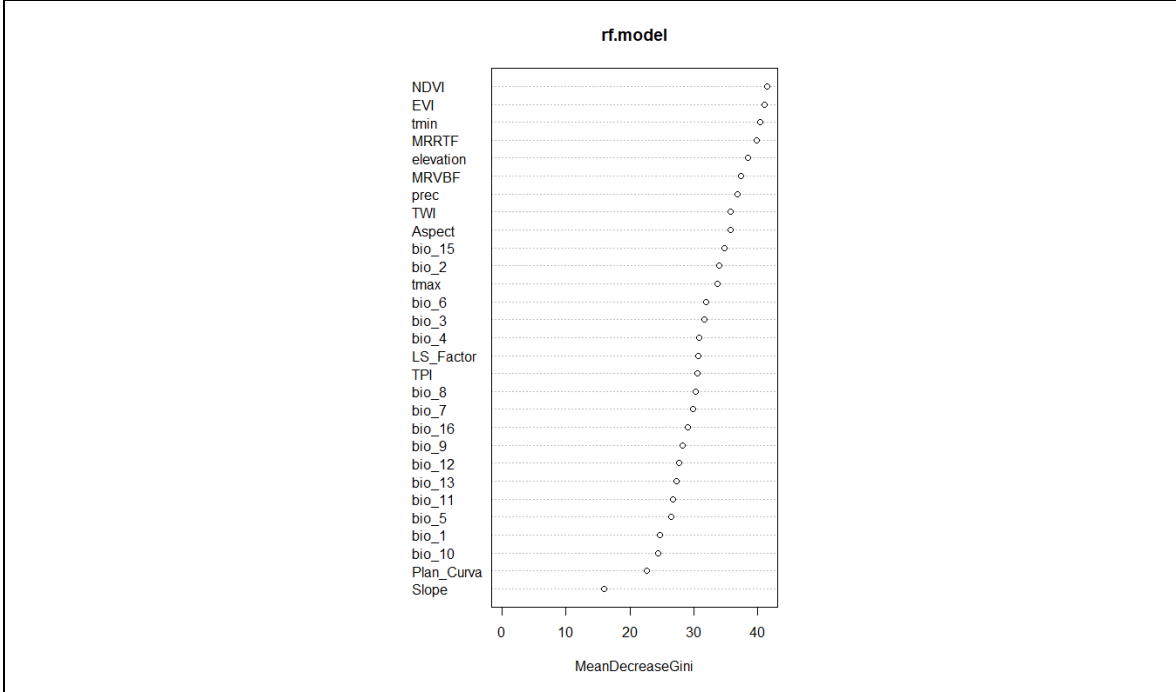
		Observed			Classification error
		Clay soils	Loamy soils	Sandy soils	
Predicted	Soil textural class				
	Clay soils	187	79	106	0.50
	Loamy soils	63	275	175	0.46
	Sandy soils	76	133	591	0.26

417

418



(a) Soil depth (b) Coarse fragments



(c) Soil texture

Fig. 3. Importance variables for prediction of soil depth (a), coarse fragment (b) and soil textural classes (c)

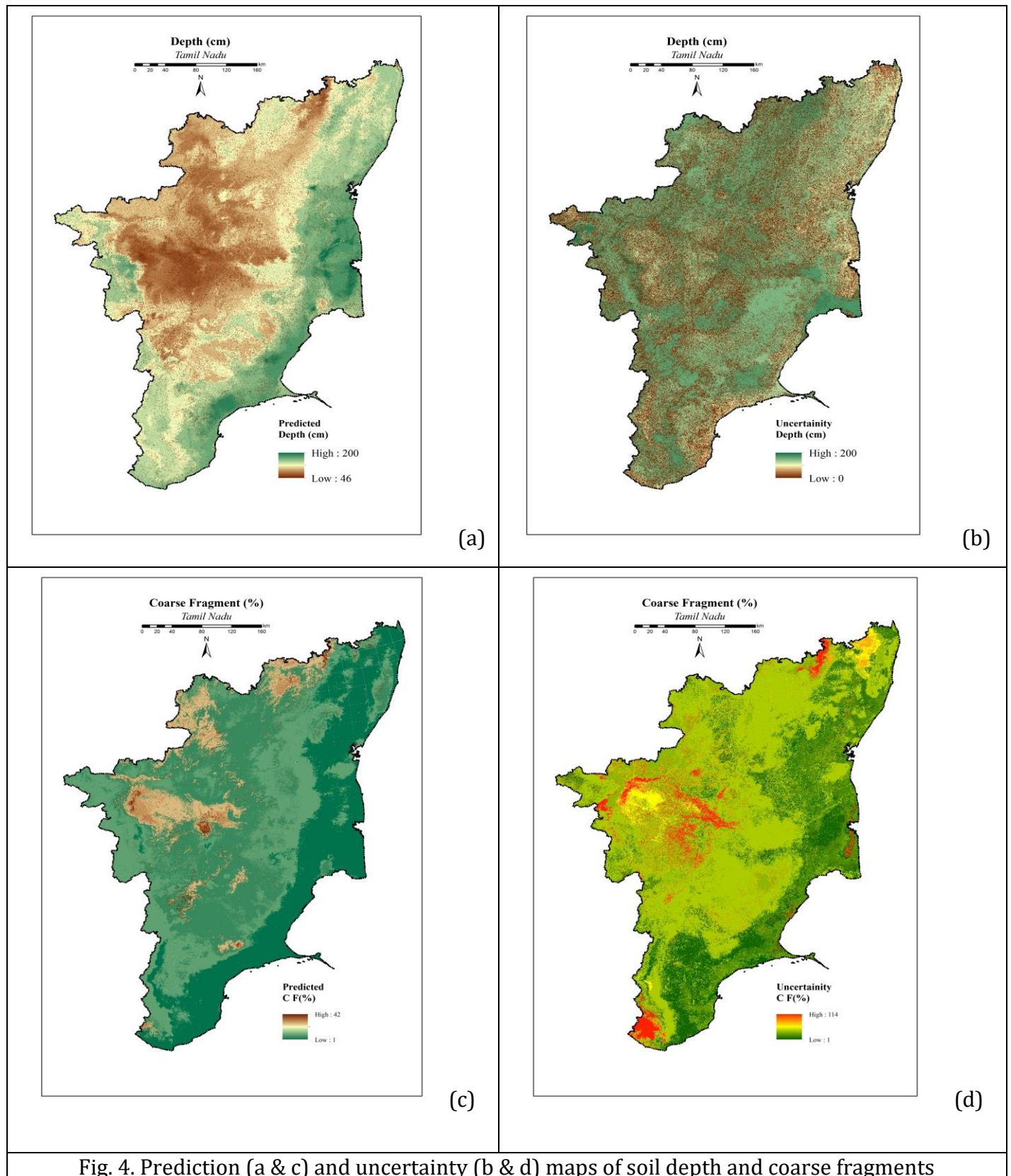


Fig. 4. Prediction (a & c) and uncertainty (b & d) maps of soil depth and coarse fragments

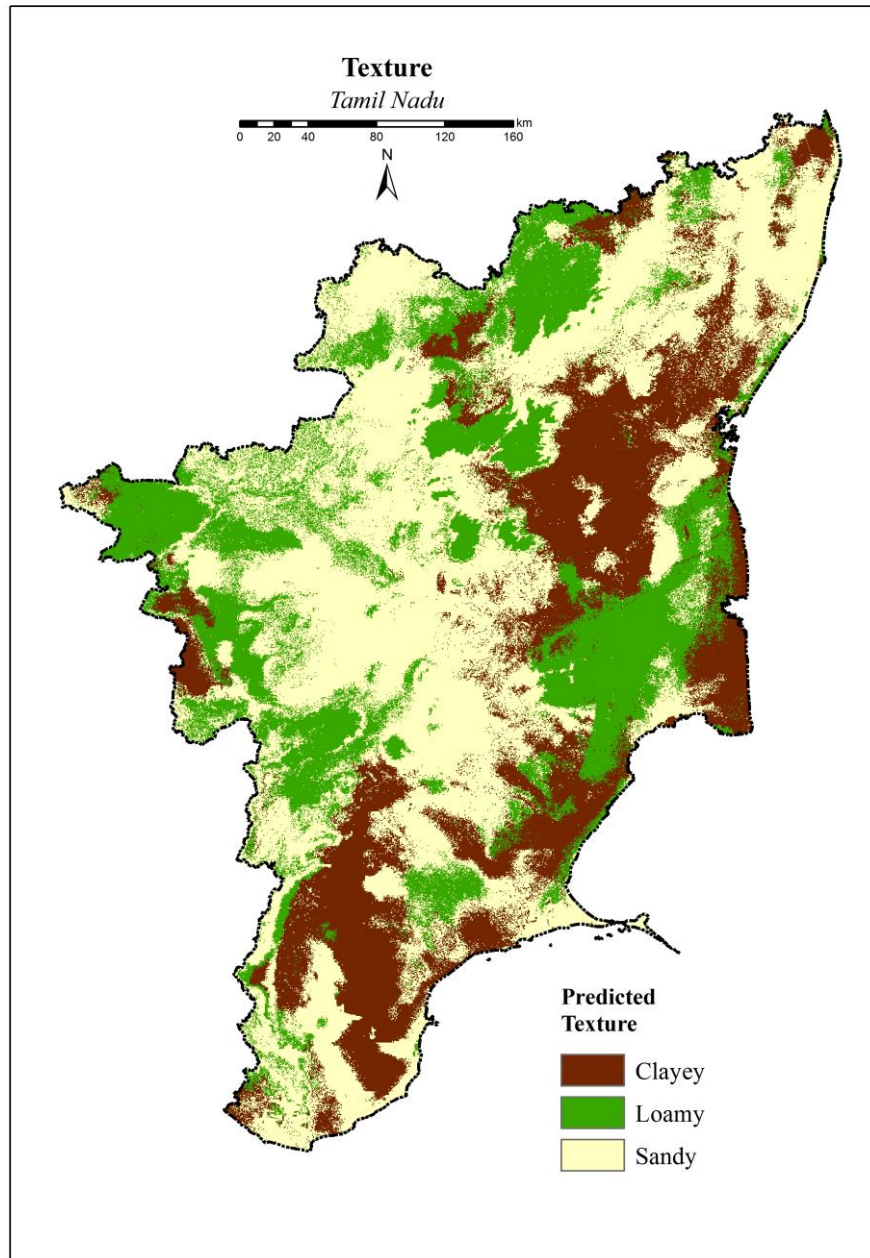


Fig. 5. Surface soil textural map of Tamil Nadu

420
421
422
423
424

425References:

- 426Abraham S, Huynh C, Vu H (2020) Classification of Soils into Hydrologic Groups Using Machine
427 Learning. Data 5: 2. doi:10.3390/data5010002
- 428Adhikari K, Kheir RB, Greve MB, Bøcher PK, Malone BP, Minasny B, McBratney AB, Greve MH
429 (2013) High-resolution 3-d mapping of soil texture in Denmark. Soil Sci Soc Am J 77:
430 860–876
- 431Akpa SIC, Odeh IOA, Bishop TFA, Hartemink AE (2014) Digital mapping of soil particle-size
432 fractions for Nigeria. Soil Sci Soc Am J 78: 1953–1966
- 433Arrouays D, Grundy MG, Hartemink AE, Hempel JW, Heuvelink GBM, Hong SY, Lagacherie P,
434 Lelyk G, McBratney AB, McKenzie NJ, Mendonça-Santos MD, Minasny B, Montanarella L,
435 Odeh IOA, Sanchez PA, Thompson JA, Zhang GL (2014) GlobalSoilMap: towards a fine-
436 resolution global grid of soil properties. Advances in Agronomy 125: 93–134
- 437Bonfatti BR, Hartemink AE, Giasson E, Tornquist CG, Adhikari K (2016) Digital mapping of soil
438 carbon in a viticultural region of Southern Brazil. Geoderma 261: 204–221.
439 <http://dx.doi.org/10.1016/j.geoderma.2015.07.016>
- 440Breiman L (2001) Random forests. Machine Learn.
441 <https://doi.org/10.1023/A:1010933404324>
- 442Byrt T, Bishop J, Carlin JB (1993) Bias, prevalence and kappa. Journal of Clinical Epidemiology
443 46(5): 423-429
- 444Camera C, Zomeni Z, Noller JS, Zissimos AM, Christoforou IC, Bruggeman A (2017) A high-
445 resolution map of soil types and physical properties for cyprus: A digital soil mapping
446 optimization. Geoderma 285: 35-49, <https://doi.org/10.1016/j.geoderma.2016.09.019>

447 Carrizo ME, Alesso CA, Cosentino D, Imhoff S (2015) Aggregation agents and structural
448 stability in soils with different texture and organic carbon contents. *Scientia Agricola*
449 72: 75-82

450 Chagas CDS, Junior WDC, Bhering SB, Filho BC (2016) Spatial prediction of soil surface texture
451 in a semi-arid region using random forest and multiple linear regressions. *Catena* 139:
452 232–240

453 Chan HC, Chang CH, Chen PA, Lee JT (2019) Using multinomial logistic regression for
454 prediction of soil depth in an area of complex topography in Taiwan. *Catena* 176: 419–
455 429

456 Cohen J (1960) A coefficient of agreement for nominal scales. *Educ Psychol Meas* 20: 37–46

457 Congalton RG, Green K (1998) *Assessing the Accuracy of Remotely Sensed Data: Principles and*
458 *Practices*. CRC/Taylor & Francis, Boca Raton, USA

459 Demattê JAM, Alves MR, Terra F da S, Bosquilia RWD, Fongaro CT, Barros PP da S (2016) Is It
460 Possible to Classify Topsoil Texture Using a Sensor Located 800 km Away from the
461 Surface? *Revista Brasileira de Ciência do Solo*, 40, e0150335

462 Dharumarajan S, Hegde R, Singh SK (2017) Spatial prediction of major soil properties using
463 Random Forest techniques-a case study in semi-arid tropics of South India. *Geoderma*
464 *Regional*, 10:154–162

465 Dharumarajan S, Kalaiselvi B, Lalitha M, Vasundhara R, Rajendra Hegde (2021) Defining
466 fertility management units and land suitability analysis using digital soil mapping
467 approach. Geocarto International. <https://doi.org/10.1080/10106049.2021.1926553>

468 Dharumarajan S, Kalaiselvi B, Suputhra A, Lalitha M, Hegde R, Singh SK, Lagacherie P (2020)
469 Digital soil mapping of key GlobalSoilMap properties in Northern Karnataka Plateau.

470 Geoderma Regional, 20. <https://www.x->
471 [mol.com/paperRedirect/1307836545166970880](https://www.x-mol.com/paperRedirect/1307836545166970880)

472Dharumarajan S, Vasundhara R, Suputhra A, Lalitha M, Hegde R (2020a) Prediction of soil
473 depth in Karnataka using digital soil mapping approach. Journal of Indian Society of
474 Remote Sensing 48(11): 1593–1600

475Dharumarajan S, Hegde R (2020b) Digital mapping of soil texture classes using Random Forest
476 classification algorithm. Soil Use and Management.
477 <https://doi.org/10.1111/sum.12668>

478Dharumarajan S, Hegde R, Janani N, Singh SK (2019) The need for digital soil mapping in India.
479 Geoderma Regional, <https://doi.org/10.1016/j.geodrs.2019.e00204>

480Boroujeni EI, Shahini-Shamsabadi M, Shirani H, Mosleh Z, Bagheri-Bodaghabadi M, Salehi MH
481 (2020) Assessment of different digital soil mapping methods for prediction of soil
482 classes in the Shahrekord plain, Central Iran. Comparison of error and uncertainty of
483 decision. Catena 193, 104648

484Florinsky I, Eilers R, Manning G, Fuller L (2002) Prediction of soil properties by terrain
485 modeling. Environmental Modelling and Software 17(3): 295–311

486Gessler PE, Moore ID, McKenzie NJ, Ryan PJ (1995) Soil landscape modelling and spatial
487 prediction of soil attributes. Int Geogr Inf Syst, 9: 421– 432.
488 doi:10.1080/02693799508902047

489Gribb M, Forkutsa I, Hansen AJ, Chandler D, McNamara J (2009) The effect of various soil
490 hydraulic property estimates on soil moisture simulations. Vadose Zone J 8:321 – 331.
491 doi:10.2136/vzj2008.0088

492Grimm R, Behrens T, Märker M, Elsenbeer H (2008) Soil organic carbon concentrations and
493 stocks on Barro Colorado Island—digital soil mapping using random forests analysis.
494 Geoderma 146: 102–113. <http://dx.doi.org/10.1016/j.geoderma.2008.05.008>

495Hengl T, Heuvelink GBM, Stein A (2004) A generic framework for spatial prediction of soil
496 variables based on regression-kriging. Geoderma 120: 75–93

497Hengl T, Miller MAE, Križan J, Shepherd KD, Sila A, Kilibarda M, Antonijević O, Glušica L,
498 Dobermann A, Haefele SM, McGrath SP, Acquah GE, Collinson J, et al (2021) African soil
499 properties and nutrients mapped at 30 m spatial resolution using two-scale ensemble
500 machine learning. Sci Rep, 11: 6130. <https://doi.org/10.1038/s41598-021-85639-y>

501Heung B, Bulmer CE, Schmidt MG (2014) Predictive soil parent material mapping at a regional-
502 scale: a Random Forest approach. Geoderma 214-215, 141–154.
503 <http://dx.doi.org/10.1016/j.geoderma.2013.09.016>.

504Heuvelink GB (2013) Uncertainty quantification of GlobalSoilMap products. Glob Basis Glob
505 Spat soil Inf Syst: 327–332

506Hillel D (1980) Applications of Soil Physics. Academic Press Inc

507Jenny H (1941) Factors of Soil Formation: A Quantitative System in Pedology, 281 pp, McGraw-
508 Hill, New York

509Kalaiselvi B, Lalitha M, Dharumarajan S, Srinivasan R, Rajendra Hegde, Anil Kumar KS, Singh SK
510 (2019) Fertility capability classification of semi-arid upland soils of Palani block, Tamil
511 Nadu for sustainable soil management. Indian Journal of Soil Conservation 47 (3): 143-
512 147

513Katerji N, Mastrorilli M (2009) The effect of soil texture on the water use efficiency of irrigated
514 crops: Results of a multi-year experiment carried out in the Mediterranean region.
515 European Journal of Agronomy 30(2): 95–100. doi:10.1016/j.eja.2008.07.009

516Kettler TA, Doran JW, Gilbert TL (2001) Simplified method for soil particle-size determination
517 to accompany soil-quality analyses. Soil Science Society of America Journal 65: 849–
518 852

519Kong X, Dao TH, Qin J, Qin H, Li C, Zhang F (2009) Effects of soil texture and land use
520 interactions on organic carbon in soils in North China cities' urban fringe. Geoderma
521 154(1-2): 86–92. doi:10.1016/j.geoderma.2009.09.016

522Kuriakose SL, Devkota S, Rossiter DG, Jetten VG (2009) Prediction of soil depth using
523 environmental variables in an anthropogenic landscape, a case study in the Western
524 Ghats of Kerala, India. Catena 79(1): 27–38

525Lacoste M, Minasny B, McBratney A, Michot D, Viaud V, Walter C (2014) High resolution 3D
526 mapping of soil organic carbon in a heterogeneous agricultural landscape. Geoderma
527 213: 296–311

528Lagacherie P, Arrouays D, Bourennane H, Gomez C, Martin M, Saby NP (2019) How far can the
529 uncertainty on a Digital Soil Map be known? A numerical experiment using pseudo
530 values of clay content obtained from Vis-SWIR hyperspectral imagery. Geoderma 337:
531 1320–1328

532Lagacherie P, McBratney AB (2007) Spatial soil information systems and spatial Soil inference
533 systems: perspectives for digital soil mapping. In: Lagacherie P, McBratney AB, Voltz M
534 (Eds), Digital Soil Mapping: An Introductory Perspective. Elsevier BV. hlm, The
535 Netherlands, pp. 3–22

536Ließ M, Glaser B, Huwe B (2012) Making use of the World Reference Base diagnostic horizons
537 for the systematic description of the soil continuum – application to the tropical
538 mountain soil-landscape of southern Ecuador. *Catena* 97: 20–30

539Lu Y, Liu F, Zhao Y, Song X, Zhang G (2019) An integrated method of selecting environmental
540 covariates for predictive soil depth mapping. *Journal of Integrative Agriculture* 18: 301–
541 315. [https://doi.org/10.1016/S2095-3119\(18\)61936-7](https://doi.org/10.1016/S2095-3119(18)61936-7)

542Mashalaba L, Galleguillos M, Seguel O, Poblete-Olivares J (2020) Predicting spatial variability of
543 selected soil properties using digital soil mapping in a rainfed vineyard of central Chile.
544 *Geoderma Regional* 22, e00289

545Malone B, Minasny B, Odgers N, McBratney AB (2014) Using model averaging to combine soil
546 property rasters from legacy soil maps and from point data. *Geoderma* 232-234, 34–44

547Malone BP, Luo Z, He D, Rossel RAV, Wang E (2020) Bioclimatic variables as important spatial
548 predictors of soil hydraulic properties across Australia’s agricultural region. *Geoderma*
549 *Regional*, e00344. doi:10.1016/j.geodrs.2020.e00344

550McBratney AB, Mendonca-Santos ML, Minasny B (2003) On digital soil mapping. *Geoderma*
551 117: 3–52. [https://doi.org/10.1016/S0016-7061\(03\)00223-4](https://doi.org/10.1016/S0016-7061(03)00223-4)

552Mehnatkesh A, Ayoubi S, Jalalian A, Sahrawat KL (2013) Relationships between soil depth and
553 terrain attributes in a semi-arid hilly region in western Iran. *J Mt Sci*, 10 (1): 163–172

554Mehrabi-Gohari E, Matinfar HR, Jafari A, Taghizadeh-Mehrjardi R, Triantafilis J (2019) The
555 Spatial Prediction of Soil Texture Fractions in Arid Regions of Iran. *Soil System* 3: 65

556Minasny B, McBratney AB (2016) Digital soil mapping: a brief history and some lessons.
557 *Geoderma* 264: 301–311

558 Mitran T, Mishra U, Lal R, Ravisankar T, Sreenivas K (2018) Spatial distribution of soil carbon
559 stocks in a semi-arid region of India. *Geoderma Regional*, e00192
560 <https://doi.org/10.1016/j.geodrs.2018.e00192>

561 Mosleh Z, Salehi MH, Jafari A, Borujeni IE, Mehnatkesh A (2016) The effectiveness of digital soil
562 mapping to predict soil properties over low-relief areas. *Environmental Monitoring and*
563 *Assessment*, 188 (195). <http://dx.doi.org/10.1007/s10661-016-5204-8>

564 Natarajan A, Reddy PSA, Sehgal J, Velayutham M (1997) Soil Resources of Tamil Nadu for Land
565 Use Planning. NBSS Publ 46b (Soils of India series) National Bureau of Soil Survey and
566 Land Use Planning, Nagpur, India p. 88 +4 sheet soil map 1:500,000 scale

567 Nussbaum M, Spiess K, Baltensweiler A, Grob U, Keller A, Greiner L, Schaepman ME, Papritz A
568 (2018) Evaluation of digital soil mapping approaches with large sets of environmental
569 covariates. *Soil* 4:1–22. <https://doi.org/10.5194/soil-4-1-2018>, 2018

570 Odeh IOA, Chittleborough DJ, McBratney AB (1991) Elucidation of soil-landform
571 interrelationships by canonical ordination analysis. *Geoderma* 49:1-32

572 Reddy NN, Chakraborty P, Roy S, Singh K, Minasny B, McBratney AB, Biswas A, Das BS (2021)
573 Legacy data-based national scale digital mapping of key soil properties in India.
574 *Geoderma*. <https://doi.org/10.1016/j.geoderma.2020.114684>

575 Rudiyanto, Minasny B, Setiawan BI, Arif C, Saptomo SK, Chadirin Y (2016) Digital mapping for
576 cost-effective and accurate prediction of the depth and carbon stocks in Indonesian
577 peatlands. *Geoderma* 272: 20–31

578 Senagi K, Jouandea N, Kamoni P (2017) Using parallel random forest classifier in predicting
579 land suitability for crop production. *Journal of Agricultural Informatics* 8(3): 23–32.
580 <https://doi.org/10.17700/jai.2017.8.3.390>

581 Shivaprasad CR, Reddy RS, Sehgal J, Velayutham M (1998) Soils of Karnataka for optimizing
582 land use. NBSS&LUP publication No.47b, Nagpur

583 Silva BPC, Silva MLN, Avalos FAP, Menezes MDD, Curi N (2019) Digital soil mapping including
584 additional point sampling in Posses ecosystem services pilot watershed, southeastern
585 Brazil. *Sci Rep Nat* 9, 13763

586 Soil Survey Staff (2014) Soil taxonomy: a basic systems of soil classification for making and
587 interpreting soil surveys (Twelfth ed). USDA, NRCS

588 Sreenivas K, Dadhwal VK, Kumar S, Harsha GS, Mitran T, Sujatha G, Suresh GJR, Fyzee MA,
589 Ravisankar T (2016) Digital mapping of soil organic and inorganic carbon status in
590 India. *Geoderma* 269: 160–173. <https://doi.org/10.1016/j.geoderma.2016.02.002>

591 Story M, Congalton R (1986) Accuracy assessment: A user's perspective. *Photogrammetric
592 Engineering and Remote Sensing* 52:397–399

593 Tesfa TK, Tarboton DG, Chandler DG, McNamara JP (2009) Modelling soil depth from
594 topographic and land cover attributes. *Water Resources Research* 45, W10438.
595 <https://doi.org/10.1029/2008WR007474>

596 Thompson JA, Roecker S, Grunwald S, Owens PR (2012) Digital soil mapping: Interactions with
597 and applications for hydrogeology, In *Hydrogeology*, edited by: Lin H, Academic
598 Press, Boston, 665-709

599 Tola E, Al-Gaadi KA, Madugundu R, Zeyada AM, Kayad AG, Biradar CM (2017) Characterization
600 of spatial variability of soil physicochemical properties and its impact on Rhodes grass
601 productivity. *Saudi Journal of Biological Sciences* 24(2): 421–429.
602 [doi:10.1016/j.sjbs.2016.04.013](https://doi.org/10.1016/j.sjbs.2016.04.013)

603 Tsai CC, Chen ZS, Duh CT, Horng FW (2001) Prediction of soil depth using a soil landscape
604 regression model: a case study on forest soils in southern Taiwan. National Science
605 Council of the Republic of China. Part B- Life Sciences 25(1): 34–39

606 Vågen TG, Winowiecki LA, Tondoh JE, Desta LT, Gumbrecht T (2016) Mapping of soil properties
607 and land degradation risk in Africa using MODIS reflectance. Geoderma 263: 216–225

608 Vaysse K, Lagacherie P (2015) Evaluating digital soil mapping approaches for mapping
609 GlobalSoilMap soil properties from legacy data in Languedoc-Roussillon (France).
610 Geoderma Regional 4: 20–30

611 Vaysse K, Lagacherie P (2017) Using quantile regression forest to estimate uncertainty of
612 digital soil mapping products. Geoderma 291: 55–64.
613 <https://doi.org/10.1016/j.geoderma.2016.12.017>

614 Viscarra Rossel RA, Webster R, Bui EN, Baldock JA (2014) Baseline map of organic carbon in
615 Australian soil to support national carbon accounting and monitoring under climate
616 change. Glob Chang Biol 20: 2953–2970

617 Wilding L (1985) Spatial variability: its documentation, accommodation and implication to soil
618 surveys. In Soil Spatial Variability Workshop, 166–194

619 Zeraatpisheh M, Ayoubi S, Jafari A, Tajik S, Finke P (2019) Digital mapping of soil properties
620 using multiple machine learning in a semiarid region, central Iran. Geoderma 338: 445-
621 452. <https://doi.org/10.1016/j.geoderma.2018.09.006>

622 Zhang M, Shi W, Xu Z (2020) Systematic comparison of five machine-learning models in
623 classification and interpolation of soil particle size fractions using different transformed
624 data. Hydrology and Earth System Science 24: 2505–2526.
625 <https://doi.org/10.5194/hess-24-2505-2020>

626

627